# Modeling and Identification of the Yaw Dynamics of an Autonomous Tractor

Erkan Kayacan, Erdal Kayacan, Herman Ramon and Wouter Saeys
Division of Mechatronics, Biostatistics and Sensors (MeBioS),
Department of Biosystems (BIOSYST),
University of Leuven (KU Leuven)
Kasteelpark Arenberg 30, B-3001 Leuven, Belgium.
E-mail: {erkan.kayacan, erdal.kayacan, herman.ramon, wouter.saeys}@biw.kuleuven.be

***Abstract*—This study deals with the yaw dynamics modeling and identification of an autonomous tractor. First, three different yaw dynamics models are developed considering various types of soil conditions. In these model derivations, the relaxation length is considered to calculate the tire side-slip angles for the two models, and the linear model is used to calculate the lateral forces on the tires for all the models. Then, to determine the most appropriate model for the autonomous tractor at hand, frequency domain identification method is preferred. After checking the level of nonlinearities of the steering mechanism and the yaw dynamics by using an odd-odd multisine signal as the excitation, these systems are identified by using maximum likelihood frequency domain identification method. The identifications results show that the two derived models among the three different models have the ability of identifying the yaw dynamics accurately. As a simpler model, an empirical second order model gives also reasonable identification results for the tractor at hand.**

## I. Introduction

Food consumption has been increasing dramatically all over the world, unlike the arable area is limited and also decreasing due to the climate change. Thus, the agricultural productivity efficiency becomes a very popular issue in today's world. Even if the productivity per hectare has increased due the fact that the capacities of the agricultural production machines have expanded, the cost of the manpower has become an economic pressure. One possible solution is the full automation of the agricultural production machines to improve the efficiency and productivity in various field operations and thus reduce the production costs.

One of the most important tasks for the machine operator is the accurate steering during the field operation to avoid damaging the crop. For instance, the rows must be parallel and the distance between them must also be equal during the planting. However, the steering accuracy decreases when the operator gets tired or does multi-tasking. As a solution, a fully autonomous and accurate control of an tractor is more than welcome. In order to be able to design an accurate model-based controller, an accurate dynamic model of the system is a must. In this study, a decent model is found for the tractor at hand by using the frequency response function (FRF) measurements.

In this study, the yaw dynamics of an autonomous tractor is derived considering various types of soil conditions and various definition of side slip angles. Then, the derived models are validated by using FRF measurements, and maximum likelihood (ML) frequency domain identification (FDI) approach is used to obtain the model parameters.

This paper is organized as follows: The experimental set-up is described in Section II. Three different mathematical models of the yaw dynamics of a tractor are given in Section III. In Section IV, the identification of the steering mechanism and the yaw dynamics is presented. Finally, a brief conclusion and future work of the study are given in Section V.

## II. Experimental Set-up

The main goal of the following experiments is to identify the steering mechanism and the yaw dynamics of an autonomous tractor for a Case New Holland (CNH) TZ25DA model which is seen in Fig. 1.

All sensors are connected to a real time operating system (PXI platform, National Instrument Corporation, USA) via a RS232 serial communication. The PXI system gathers the steering angle and the yaw rate measurements, then controls them by sending the proper messages to actuators. A PC is connected to the PXI system via wireless connection, and it also functions as the user interface of the autonomous tractor. All the algorithms are implemented in $LabVIEW^{TM}$ version


Fig. 1. The experimental set-up (CNH TZ25DA)

978-1-4673-5769-2/13/$31.00 ©2013 IEEE

2011, National Instrument, USA. They are executed in real-time on the PXI and updated at a rate of 20-Hz and 200-Hz for the outer loop (yaw dynamics control) and the inner loop (steering control), respectively.

In the inner closed loop, the steering mechanism is controlled by using an electro-hydraulic valve from Sauer Danfoss with a flow rate of 12 liter/min. The electro-hydraulic valve characteristics are highly nonlinear, and they have saturation and a dead-band regions. The voltage given to the actuator is limited between $0-12$ volt and the steering angle is also limited in the interval of $\pm 45^{\circ}$. The former signal is the input and the latter signal is the output of the steering system, respectively. The position of the front wheels is measured using a potentiometer mounted on the front axle yielding a position measurement resolution of $1^{\circ}$. Moreover, the yaw rate of the tractor is measured using a gyro yielding a measurement resolution of $1^{\circ}$/s.

## III. Modeling of the Yaw Dynamics of a Tractor

The velocities, the sideslip angles and the forces at the rigid body of an autonomous tractor are presented in Fig. 2. The yaw dynamics models are derived based-on the following assumptions:

- The longitudinal speed is constant,
- The traction, the tire-road friction and the aerodynamic forces are neglected,
- Since the tire moments are too small, they are neglected;
- The steering angle is small,
- The pitch and roll dynamics are neglected.

The notations used in the sequel (see also Fig. 2) are shown in Table I as follows:

TABLE I. NOMENCLATURE

| | |
|---|---|
| $m$ | Mass of the tractor |
| $I$ | Moment of inertia of the tractor around the vertical axis |
| $v_x$ | Longitudinal velocity of the center of the gravity of the tractor |
| $v_y$ | Lateral velocity of the center of the gravity of the tractor |
| $\psi$ | Yaw angle of the tractor |
| $\gamma$ | Yaw rate of the tractor |
| $\delta$ | Steering angle of the front wheels |
| $l_f$ | Distance between the front axle and the center of the gravity of the tractor |
| $l_r$ | Distance between the rear axle and the center of the gravity of the tractor |
| $L$ | Distance between the front axle and the rear axle of the tractor |
| $F_{t,f}$, $F_{t,r}$ | Traction forces on the front and the rear wheels of the tractor, respectively |
| $F_{l,f}$, $F_{l,r}$ | Lateral forces on the front and the rear wheels of the tractor, respectively. |
| $C_{\alpha,f}$, $C_{\alpha,r}$ | Cornering stiffness of the front and rear wheels of the tractor, respectively |
| $\alpha_f$, $\alpha_r$ | Side slip angles of the front and rear wheels of the tractor, respectively |
| $\sigma_f$, $\sigma_r$ | Relaxation lengths of the front and rear wheels of the tractor, respectively |

### A. Vehicle Dynamics

The longitudinal motion of the tractor is written as follows:

$$m(\dot{v}_x - v_y\gamma) = F_{t,f}\cos\delta - F_{l,f}\sin\delta + F_{t,r} \tag{1}$$

where $m$, $F_{t,f}$, $F_{l,f}$, $F_{t,r}$ represent the mass of the tractor, the traction and lateral forces on the front wheel, the traction force on the rear wheel, respectively.

The lateral motion of the tractor is written as follows:

$$m(\dot{v}_y + v_x\gamma) = F_{t,f}\sin\delta + F_{l,f}\cos\delta + F_{l,r} \tag{2}$$

where $F_{l,r}$ represents the lateral force on the rear wheel.

The yaw motion of the tractor is written as follows:

$$I\dot{\gamma} = l_f(F_{t,f}\sin\delta + F_{l,f}\cos\delta) - l_rF_{l,r} \tag{3}$$

where $l_f, l_r$ and $I$ represent the distance between the front axle and the center of the gravity of the tractor, the distance between the rear axle and the center of the gravity of the tractor, the moment of inertia of the tractor. An estimated yaw inertia of the tractor can be calculated approximately as follows [1]:

$$I = ml_fl_r \tag{4}$$

### B. Tire Model

The lateral tire forces are calculated in a linear model which assumes to be proportional to the slip angles in [2], [3]

$$F_{l,i} = -C_{\alpha,i}\alpha_i \qquad i = \{f, r\} \tag{5}$$

where $C_{\alpha,i}$ and $\alpha_i$ $i = \{f, r\}$, represent cornering stiffness of the tires and side-slip angles, respectively. The tire cornering stiffness parameters are an averaged slope of the lateral force characteristic in this method.

The tire side slip angles must be calculated in order to determine the slip forces. The side slip angles of the front and rear tires are written as follows:

$$\begin{aligned} \alpha_f &= \frac{v_y + l_f\gamma}{v_x} - \delta \\ \alpha_r &= \frac{v_y - l_r\gamma}{v_x} \end{aligned} \tag{6}$$

The relaxation length is defined as the amount a tire rolls to reach steady state side slip angle. As can be seen from previous

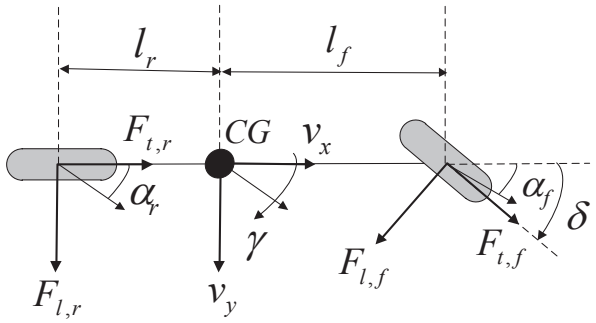


Fig. 2. Dynamics bicycle model for a tractor system: velocities, side slip angles and forces at the rigid body of the system

researches in agricultural vehicles, the relaxation length of a tire plays a very important part in steering motion at high velocities [4], [5]. Since a tire generates the steady state side slip angle simultaneously, a first order mathematical model is used to describe the slip angle dynamics through relaxation length. The side slip angle is written as follows:

$$\dot{\alpha} = \frac{u}{\sigma}(\alpha_0 - \alpha) \tag{7}$$

The relaxation length for agricultural vehicles is determined 1.5 times the tire radius to obtain the similar changes at the same amount increase in velocity [6]. As can be seen from past researches, since passenger vehicles have higher velocity than agricultural vehicles, it is selected bigger than twice [7].

The two side slip angles of the tires are written as follows:

$$\dot{\alpha}_f = \frac{v_y + l_f\gamma - v_x(\delta + \alpha_f)}{\sigma_f} \tag{8}$$

$$\dot{\alpha}_r = \frac{v_y - l_r\gamma - v_x\alpha_r}{\sigma_r} \tag{9}$$

where $\sigma_f$ and $\sigma_r$ represent the relaxation length of the front and rear tires of the tractor, respectively.

### C. Equations of Yaw Motion

The tractor is driven on the field with a constant longitudinal velocity as required in automatic guidance of agricultural vehicles. Therefore, longitudinal slip occurs only when the system is accelerating or decelerating. Consequently, the traction forces can be neglected and the time derivative of longitudinal velocity $u_c^t$ will be equal to zero. It is also assumed that the steering angle is sufficiently small to obtain linearized equations. Thus, (2) and (3) are written considering (5) as follows:

$$\begin{aligned} m\dot{v}_y &= -mv_x\gamma - C_{\alpha,f}\alpha_f - C_{\alpha,r}\alpha_r \\ I\dot{\gamma} &= -l_fC_{\alpha,f}\alpha_f + l_rC_{\alpha,r}\alpha_r \end{aligned} \tag{10}$$

Firstly, the traditional bicycle model for the yaw motion of the autonomous tractor can be written by using (6) and (10). The relation between the yaw rate of the autonomous tractor and the steering angle of the front wheels can be written in the transfer function form as follows:

$$G_{TB}(s) = \frac{b_1^\star s + b_0^\star}{a_2^\star s^2 + a_1^\star s + a_0^\star} \tag{11}$$

Secondly, the bicycle model with the relaxation length approach for the front and the rear wheels can be written by using (8), (9) and (10). The relation between the yaw rate of the autonomous tractor and the steering angle of the front wheels can be written in the transfer function form as follows:

$$G_{RLFR}(s) = \frac{b_2^* s^2 + b_1^* s + b_0^*}{a_4^* s^4 + a_3^* s^3 + a_2^* s^2 + a_1^* s + a_0^*} \tag{12}$$

Thirdly, the bicycle model with relaxation length approach for only the front wheel can be written by using (8) and (10). The relation between the yaw rate of the autonomous tractor and the steering angle of the front wheels can be written in transfer function form as follows:

$$G_{RLF}(s) = \frac{b_1^\diamond s + b_0^\diamond}{a_3^\diamond s^3 + a_2^\diamond s^2 + a_1^\diamond s + a_0^\diamond} \tag{13}$$

The different models might be proper for different real-time systems. It will be determined later the most appropriate model for the real-time system at hand.

## IV. Identification

In this part of the study, the identification of the steering mechanism is done in Section IV-B, and Section IV-C presents the comparison between the three models in Section III-C and FRF measurements of the experimental set-up.

### A. Maximum Likelihood Estimation

After decision of the order of the transfer function, a frequency domain maximum likelihood estimator is proposed in order to identify model parameters from input-output FRF measurements. Frequency domain ML estimation method considers errors-in-variables model due to process disturbance and noise on input and output measurements [8]. The Fourier coefficients of the measured input $U_m(k)$ and the measured output $Y_m(k)$ are respectively written as follows:

$$\begin{aligned} U_m(k) &= U + N_u \\ Y_m(k) &= GU + N_y \end{aligned} \tag{14}$$

where G is the transfer function of the process. Since the Fourier spectra in practice are calculated via a discrete Fourier transform, it is assumed that $N_u$ and $N_y$ are independent zero mean complex Gaussian random variables [9]. The real and imaginary parts are independent and the variance of them are equal.

A Gaussian likelihood function, which gives the probability of obtaining the set of measurements $U_m(k)$ and $Y_m(k)$ for a given set of values of the Fourier coefficients $U(k)$ and $Y(k)$, is constructed [10]. The likelihood function is a function of the unknown input and the unknown output Fourier coefficients $U(k)$ and $Y(k)$ which are related to the model parameters as follows:

$$G(\Omega_k, \theta) = \frac{Y(k)}{U(k)} \tag{15}$$

The goal is to estimate the parameter vector $\theta$ with respect to the exact Fourier coefficients via the constraint (15). The maximum likelihood cost function [11] is written as follows:

$$V_{ML}(\theta, Z_m) = \sum_{k=1}^{N} \frac{|B(\Omega_k,\theta)U_m(k) - A(\Omega_k,\theta)Y_m(k)|^2}{2Se_k^2} \tag{16}$$

where $Z_m$ and $Se_k^2$ equal to

$$Z_m = [U_{r_m}\ U_{i_m}\ Y_{r_m}\ Y_{i_m}]^T \tag{17}$$

$$\begin{aligned} Se_k^2 = {} & \sigma_u^2|B(\Omega_k,\theta)|^2 + \sigma_y^2|A(\Omega_k,\theta)|^2 \\ & -2\Re((p_r(k) + jp_i(k))A(\Omega_k,\theta)B^*(\Omega_k,\theta)) \end{aligned} \tag{18}$$

As can be seen from (16), the numerator and the denominator describe the sum of the squares of the equation error at frequency $\Omega_k$ and the variance of the equation error, respectively. Moreover, the maximum likelihood cost function is invariant with respect to the model parameters and minimized by the exact model parameters $\theta$.

### B. Identification of the Steering Mechanism

The valve characteristics for the steering system are highly nonlinear, and it includes a saturation and a dead-band region. Thus, several data sets are collected to learn the steady state characteristics of the steering valve. A model from volt-to-volt in (19) has been used to invert the nonlinear characteristics of the steering valve. Once the steady state characteristic of the steering actuator is known, it is assumed that the valve nonlinearity is perfectly inverted. The used volt-to-volt transformation (VVT) is written as follows:

$$\text{VVT} = \begin{cases} \text{if } V_i < 0 & V_o = V_i + 5.1 \\ \text{if } V_i > 0 & V_o = V_i + 6.9 \\ \text{if } V_i = 0 & V_o = 6 \end{cases} \tag{19}$$

where $V_i$ and $V_o$ are the input and the output of the VVT, respectively.

It is observed that the front wheels reach to their limits when a signal is applied to the steering mechanism an open-loop fashion. As a solution to this drifting problem, the system is controlled by a P controller and then the closed-loop system is identified. The closed loop schematic diagram of the steering mechanism is shown in Fig. 3.

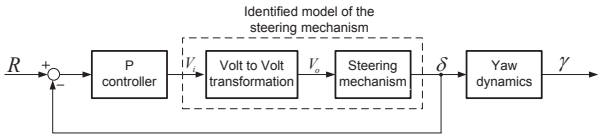


Fig. 3. The schematic diagram of the the steering mechanism in a closed-loop fashion

The steering mechanism with/out proposed VVT is excited with an odd-odd multisine to detect the level of nonlinear distortions [12], [13]. In this technique, only a well chosen set of frequency lines with a periodic excitation is excited. The rest of the frequency lines are not excited intentionally. The linear contribution and the nonlinear distortions appear in the frequencies lines as explained below:

- At lines 4k+1: Linear contribution plus nonlinear distortions
- At lines 4k+2: Only even nonlinear distortions
- At lines 4k+3: Only odd nonlinear distortions
- At lines 4k+4: Only noise

As can be seen from the output spectrum of the system given in Fig. 4, the odd-odd nonlinear contributions at the detection frequency components after VVT are smaller than the contributions at the detection lines before VVT. Figure 5 shows even nonlinear contributions at the detection frequency components in two cases. It can be seen that the level of even nonlinearities are similar.

Figure 6 shows the frequency spectrum of the response of the steering mechanism with VVT to a random odd-odd multisine excitation. It can be seen that the level of nonlinearities are similar to the level of noise and the nonlinear contributions are about 25 $dB$ smaller than linear contributions

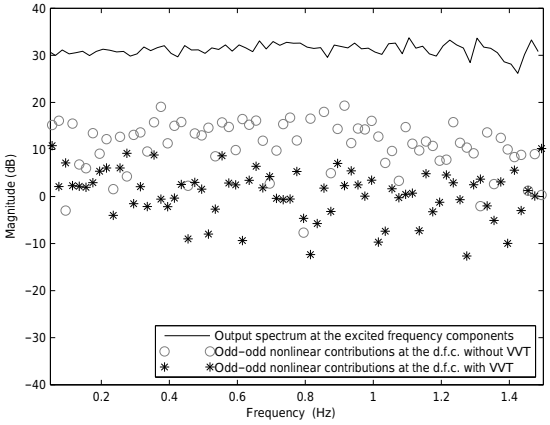


Fig. 4. The analysis of odd-odd nonlinear contributions

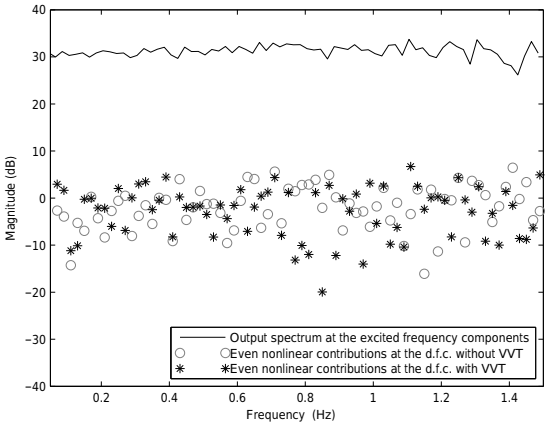


Fig. 5. The analysis of even nonlinear contributions

in the excited frequency band. This implies that the steering mechanism can be approximated by a linear model.

The steering mechanism is a high-order model. Since the natural frequency of the valve is higher than the natural frequency of the steering system, it is possible to simplify the model of the steering mechanism as a first order model for the rate of the steering angle and second order system model for the steering angle. As a result, the steering mechanism is considered as a mass-damper system for the steering angle. The relation between the voltage to the actuator and the the steering angle is modeled as:

$$\frac{\delta(s)}{V(s)} = \frac{K}{s(\tau s + 1)} \tag{20}$$

The transfer function for the closed-loop system is written as follows:

$$\frac{\delta(s)}{R(s)} = \frac{PK}{s(\tau s + 1) + PK} \tag{21}$$

where the P controller coefficient is set to $5$ in the experiments.

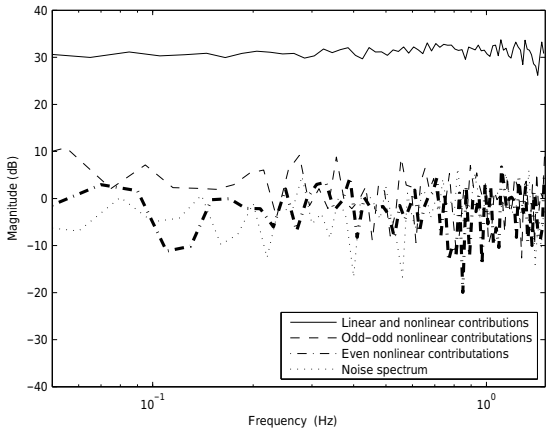


Fig. 6. The analysis of nonlinear contributions

A multisine signal with a frequency content between 0.015 Hz and 1.5 Hz is applied to the steering mechanism as an excitation signal. These parameters of the model are identified by using ML frequency domain identification approaches based on FRF measurements. Fig. 7 shows the measured FRF and the FRF of identified model in the closed-loop fashion. It is observed during the experiments that it is inconvenient to give an excitation signal to the steering system bigger than 1.5 Hz. However, the range until 1.5 Hz is enough to capture the second order peak at 0.8 Hz.

After the identification process, the transfer function of the identified model in the closed-loop fashion is calculated as follows:

$$\frac{\delta(s)}{R(s)} = \frac{43}{s^2 + 7.7s + 45} \tag{22}$$

As can be seen from (22), $PK$ values in the numerator and in the denominator are not same due to the assumption of perturbation effect. $PK$ value in denominator is used to determine the transfer function of the steering mechanism. By using (22), the transfer function of the steering mechanism with VVT is obtained as follows:

$$G(s) = \frac{\delta(s)}{V_i(s)} = \frac{1.1705}{s(0.13s + 1)} \tag{23}$$

### C. Identification of the Yaw Dynamics

Figure 8 shows the frequency spectrum of the response of the yaw rate to a random odd-odd multisine excitation. It can be seen that the contribution of the nonlinearities to total response is as large as the linear contribution after 2 Hz. As a result, a linear model can be derived between 0.02 Hz and 2 Hz.

A multisine signal with a frequency content between 0.02Hz and 2Hz is applied to the system as an excitation signal. These parameters of the model are identified by using a ML frequency domain identification approach based on FRF measurements. Figure 9 shows the measured FRF and the FRF of identified models. As can be seen from Fig. 9, since the traditional bicycle model in (11) consists of one zero and two poles, it is not a candidate for the parameter estimation.

After the identification process, the transfer functions of the identified yaw dynamics model are calculated respectively for the bicycle model with relaxation length approach for only the front wheel, the bicycle model with relaxation length approach for the front and the rear wheels, and a second order system as follows:

$$G_{RLF}(s) = \frac{265s + 27.8}{s^3 + 10.5s^2 + 225.5s + 24.25} \tag{24}$$

$$G_{RLFR}(s) = \frac{267s^2 + 55.4s + 22490}{s^4 + 10.6s^3 + 312s^2 + 923s + 19040} \tag{25}$$

$$G_{2nd}(s) = \frac{264.5}{s^2 + 10.3s + 224} \tag{26}$$

Even if the models derived in (12) and (13) fit with the real-time FRF measurements well, these models are higher order transfer functions. As a simplified empirical model, a second order transfer function in (26) is fitted to FRF measurements.

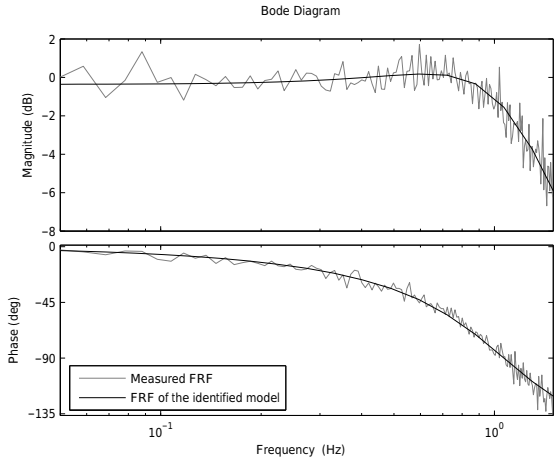


Fig. 7. Measured FRF and FRF of the identified model

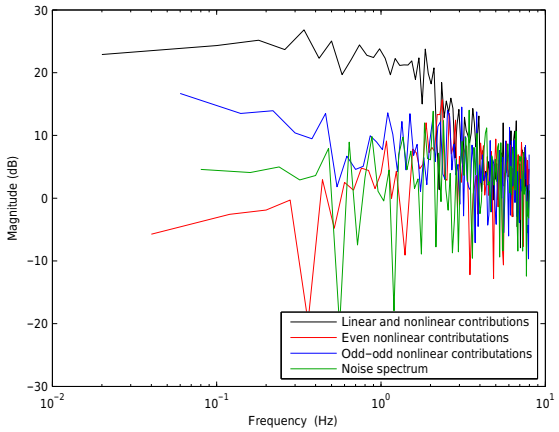


Fig. 8. The analysis of nonlinear contributions

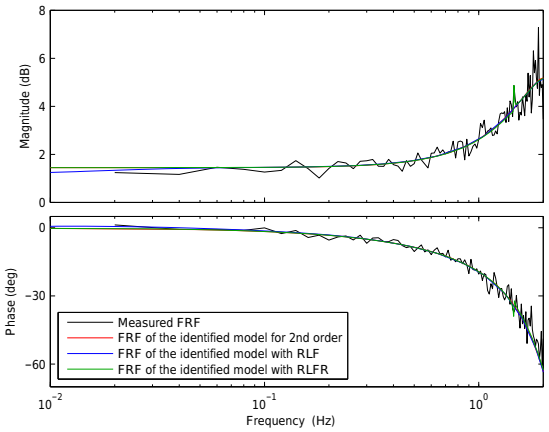


Fig. 9. Measured FRF and FRF of the identified models

As can be seen from Fig. 9, the frequency domain responses of the proposed transfer function in (26) is similar to the derived models in (24) and (25). It can be concluded that an empirical second order transfer function can also be used to model the yaw dynamics of the tractor at hand.

## V. Conclusion and Future Work

### A. Conclusion

In this study, modeling and identification aspects of an autonomous tractor are investigated. The equations of yaw motion have been derived using Newton method. Necessary assumptions are made in order to obtain a simpler dynamics model. After obtaining the identification results, it has been observed that the bicycle model with relaxation length approach for only the front wheel, the bicycle model with relaxation length approach for the front wheel and the rear wheel, and an empirical second order transfer function are proper models suited to FRF measurements. On the other hand, the traditional bicycle model is not convenient for the tractor at hand. The identification results show also that the proposed empirical second order transfer function can model the yaw dynamics of the tractor as accurate as the models derived using Newton method.

### B. Future Work

In addition to the use of a stochastic identification method (ML), a deterministic identification method such as nonlinear least square frequency domain identification method will be used. The different transfer functions coming from different estimation method will be compared. Based-on the obtained identified models, a model based-controller will be designed for the yaw dynamics of the tractor at hand.

## Acknowledgment

This work has been carried out within the framework of projects IWT-SBO 80032 (LECOPRO) of the Institute for the Promotion of Innovation through Science and Technology in Flanders (IWT-Vlaanderen). We would like to thank Mr. Soner Akpinar for his technical support for the preparation of the experimental set up.

## References

[1] W. R. Garrott, M. W. Monk, and J. P. Chrstos, "Vehicle inertial parametersmeasured values and approximations," in *SAE Passenger Car Meeting and Exposition*, Detroit, MI, 1998.

[2] D. Piyabongkarn, R. Rajamani, J. A. Grogg, and J. Y. Lew, "Development and experimental evaluation of a slip angle estimator for vehicle stability control," *IEEE Transactions on Control Systems Technologhy*, vol. 17, no. 1, pp. 78 – 88, 2009.

[3] C. Geng, L. Mostefai, M. Dena, and Y. Hori, "Direct yaw-moment control of an in-wheel-motored electric vehicle based on body slip angle fuzzy observer," *IEEE Transactions on Industrial Electronics*, vol. 56, no. 5, pp. 1411 – 1419, 2009.

[4] D. A. Crolla, "The steering behavior of off-road vehicles," in *Proceedings of 8th IAVSD-Symp.*, Cambridge, MA,, 1983.

[5] R. H. Owen and J. E. Bernard, "Directional dynamics of a tractor-loader-backhoe," *Vehicle System Dynamics*, vol. 11, pp. 251 – 265, 1982.

[6] D. M. Bevly, J. C. Gerdes, and B. W. Parkinson, "A new yaw dynamic model for improved high speed control of a farm tractor," *Journal of Dynamic Systems, Measurement, and Control*, vol. 124, pp. 659 – 667, 2002.

[7] J. Loeb, D. Guenther, and H. Chen, "Lateral stiffness, cornering stiffness, and relaxation length of the pneumatic tire," in *SAE International Congress and Exposition*, Detroit, MI, 1990.

[8] R. Pintelon, P. Guillaume, Y. Rolain, J. Schoukens, and H. Van hamme, "Parametric identification of transfer functions in the frequency domain-a survey," *Automatic Control, IEEE Transactions on*, vol. 39, no. 11, pp. 2245 –2260, nov 1994.

[9] D. Brillinger, *Time series: data analysis and theory*. Society for Industrial Mathematics, 2001, vol. 36.

[10] L. Clijmans, J. Swevers, J. D. Baerdemaeker, and H. Ramon, "Sprayer boom motion, part 1: Derivation of the mathematical model using experimental system identification theory," *Journal of Agricultural Engineering Research*, vol. 76, no. 1, pp. 61 – 69, 2000.

[11] R. Pintelon and J. Schoukens, "Robust identification of transfer functions in the s- and z-domains," *Instrumentation and Measurement, IEEE Transactions on*, vol. 39, no. 4, pp. 565–573, 1990.

[12] K. Vanhoenacker and J. Schoukens, "Detection of nonlinear distortions with multisine excitations in the case of nonideal behavior of the input signal," *Instrumentation and Measurement, IEEE Transactions on*, vol. 52, no. 3, pp. 748 – 753, 2003.

[13] J. Schoukens, R. Pintelon, T. Dobrowiecki, and Y. Rolain, "Identification of linear systems with nonlinear distortions," *Automatica*, vol. 41, no. 3, pp. 491 – 504, 2005.